The Synchronous Fitting of Cyclo-non-Stationary Signals: Definition and Theoretical Analysis

Dany Abboud[1(✉)], Amadou Assoumane[1], and Mohammed Elbadaoui[1,2]

[1] Safran Tech, Rue des Jeunes Bois - Châteaufort, 78772 Magny-les-Hameaux, France
d-abboud@live.com, dany.abboud@safrangroup.com
[2] Univ Lyon, Univ Jean-Monnet of Saint-Etienne, LASPI, EA3059, 42023 Saint-Etienne, France

Abstract. This paper addresses the problem of deterministic/random separation in vibration signals when the machine is operating under nonstationary regime. The solution to this problem is well established in the stationary regime case, where the deterministic component is simply periodic. In this regard, the synchronous average provides an optimal way to separate a deterministic synchronous source from other interferences. However, synchronous averaging theoretically requires the machine to operate under stationary regime (i.e. the related vibration signals are cyclostationary) and is otherwise jeopardized by the presence of amplitude and phase modulations. The local synchronous fitting presents a powerful generalization of the synchronous average to the non-stationary regime case (i.e. the related vibration signals are cyclo-non-stationary). The idea is to replace the (cyclic) empirical average operation by a (cyclic) local curve fitting using the Savitsky-Golay algorithm. This paper studies the temporal and spectral properties of this filter, and demonstrates its potentiality on real-world helicopter data recorded under varying operating speed.

Keywords: Gears · Bearing · Diagnosis · Nonstationary conditions · Vibration signal · Savitzky–Golay filter · Signal separation

1 Introduction

Vibratory health monitoring of rotating machines has been widely used in industries for decades. It consists in analyzing the vibration signal in order to extract machine health indicators. By its rotary movement, a machine generates a vibration signal rich in information on the health state of each of these organs including gears, bearings, shafts, fan blades etc. These signals are cyclic in nature and can be described within the cyclo-non-stationary (CNS) framework. The CNS framework extends the cyclo-stationary theory to the case where machine signals are recorded under varying operating regimes (varying load and/or speed).

F. Chaari et al. (Eds.): WNSTA 2021, ACM 18, pp. 178–192, 2022.
https://doi.org/10.1007/978-3-030-82110-4_9

They can be classified mainly into two categories: CNS at order 1 and CNS at order 2 (or higher). With regard to bearings, their characteristic signal is CNS2 in nature. In fact, when they are defective, they generate a series of random but pseudo-periodic pulses due to the sliding phenomenon in the bearing rolling elements motion [1]. In the case of gearboxes, the meshing signal is intrinsically deterministic and, thus, CNS1 in nature. Such a signal can be modeled as a sum of a sinusoid modulated by the time-varying amplitudes and phases related to the regime. For an accurate diagnosis, the separation of the CNS1 and CNS2 signals is required.

The few separation approaches in the literature using the cyclic behavior of mechanical organs are based on the estimation of the CNS1 sinusoid, generally described by sinusoidal components. Synchronous averaging is probably the most used technique for extracting sinusoidal components because of its simplicity and ease of implementation [2,3]. Despite its widespread use, it is only valid in stationary regime (constant speed and load). In variable regime, the synchronous average fails due to the structural change in the signal statistics across the cycles. In fact, the change in operating regime induces relatively slow amplitude modulations in the signal as well as phase modulations. Methods adapted to the analysis of non-stationary signals are present in the literature. Previously, there was an attempt to generalize the SA by Daher et. *al* [4] using a parametric approach. In details, the authors decomposed the deterministic components onto a set of periodic functions multiplied by functions dependent on the speed capable of capturing long-term evolution over consecutive cycles. This approach uses a higher-order polynomial to estimate the sinusoidal component throughout the cycle contained in the raw vibration signal. It was shown that this technique suffers from side effects and underestimates the entire dynamic of the sinusoidal component.

Also, It is worth mentioning that authors in [5] proposed the so-called "Generalized Synchronous Average", denoted GSA, for the variable speed condition. A particular difference between the GSA and the proposed approach, is the fact that the applicability of the former is confined to the case where only one CNS agent varies during the acquisition (e.g. speed or torque) and its profile has to be known. In fact, the GSA decomposes the CNS agent profile into a given number of regimes and perform the average for each regime. A commonly encountered scenario in rotating machine is when the speed and load vary simultaneously. In this case, the GSA is not applicable whereas the proposed method can deal with this issue.

Recently, the so-called local synchronous fitting (LSF) [6] has been proposed. The LSF uses a lower order polynomial to estimate the complex envelope across the cycles. In reference [6] the LSF showned to perform better than the method proposed by Daher et *al.* [4].
Other parametric methods such as Vold-Kalman filtering [7], H_∞ filtering [8], biquadratic filtering [9] have been proposed to monitor rotating machines under variable speed conditions.

For the time being, the properties of the LSF are not studied. The aim of this paper is to fill this gap by studying the time and frequency properties of the LSF filter. The paper is organized as follows. In Sect. 2 we recall the LSF for the estimation of sinusoidal components. In Sect. 3 the properties in time and frequency domain of the LSF filter is studied. In Sect. 4 the LSF filter is applied to analyze a helicopter vibration signal. The last section concludes the paper.

2 Polynomial Generalization of the Synchronous Average

2.1 Cyclo-non-Stationary Signals

Cyclo-non-stationary (CNS) signals are firstly proposed to describe vibration signals recorded under strong varying regimes. These signals, though being resampled in the angular domain, present strong long-term statistical change in their structure that prevents them to be cyclostationary. As it will be shown in this paper, the CNS class can enfold other types of signals generated from different applications, not only vibrations recorded under nonstationary regimes. As this paper is concerned with the estimation of the deterministic component, first-order CNS signals are of concern. It is proposed to define a first-order CNS signal, say $x[n]$, with a fundamental period N (i.e. cycle and $1/N$ the normalized frequency) and a length L as:

$$(\forall n \in \{1, \cdots, L\}) \quad x[n] = d[n] + w[n] = \sum_k d_k[n] e^{j2\pi kn/N} + w[n] \tag{1}$$

where k is an integer, $d_k[n] \in \mathbb{C}$ are deterministic smooth functions (whose real and imaginary part are continuous and differentiable) and whose bandwidths, denoted B_k, are much smaller than the half of the fundamental frequency i.e.: $(\forall k), B_k \ll 1/2N$ and $w[n]$ is a random noise that can possibly comprise other higher-order CNS components. The fundamental period N can be also referred to as "revolution" or "cycle". As periodicity is generally defined in the angular domain, the index n generally refers to the discret angular variable, that is $x(\theta_n) = x(n\Delta\theta) = x[n]$ where θ and $\Delta\theta$ respectively denotes the continuous angle variable and increment (angular sampling period). According to the Weirstrass theorem, the complex envelopes, $d_k[n]$, can be approximated through a P-order polynomial function, i.e.:

$$(\forall k) \quad d_k[n] \approx \sum_{p=0}^{P} d_k^p n^p \tag{2}$$

where $d_k^p \in \mathbb{C}$. By inserting Eq. (2) into the expression of $d[n]$, one obtains:

$$(\forall n \in \{1, \cdots, L\}) \quad d[n] = \sum_{p=0}^{P} c_p[n] n^p \tag{3}$$

where $c_p[n] = \sum_k d_k^p e^{j2\pi kn/N}$ is a periodic function of period N. Equation (3) indicates that the deterministic component can be approximated by a sum of

periodic functions multiplied with the polynomial basis: it is actually a polynomial with periodic coefficients.

Let us first define $\bar{n} = \lfloor n-1/N \rfloor + 1$ as the sample location within the period N (a/b denotes the division of a by b). Since $c_p(n)$ is periodic with period N, we have $c_p[\bar{n}] = c_p[\bar{n} + (q-1)N]$ for all integer $q \in \{1, \ldots, Q\}$ (Q is the number of cycles). Thus, Eq. (3) can be equivalently written as follows:

$$(\forall q \in \{1, \cdots, Q\})\,(\forall \bar{n} \in \{1, \cdots, N\}) \quad d[\bar{n}+(q-1)N] = \sum_{p=0}^{P} c_p[\bar{n}](\bar{n}+(q-1)N)^p \tag{4}$$

Using the binomial theorem $(\bar{n} + (q-1)N)^p = \sum_{i=0}^{p} C_i^p N^i (\bar{n} - N)^{p-i} q^i$ where C_i^p is the binomial coefficient), one can deduce from Eq. (4) that the samples associated with the same location $\bar{n}$ in the period, $s_q[\bar{n}] = d[\bar{n} + (q-1)N]$ for all integer $q \in \{1, \cdots, Q\}$, define a polynomial of order P with constant coefficients, i.e.:

$$(\forall q \in \{1, \cdots, Q\})\,(\forall \bar{n} \in \{1, \cdots, N\}) \quad s_q[\bar{n}] = \sum_{p=0}^{P} b_p[\bar{n}] q^p \tag{5}$$

where $b_p[\bar{n}] = N^p \sum_{j=p}^{P} C_p^j (\bar{n}-N)^{j-p} c_j[\bar{n}]$. Note that $b_p[\bar{n}]$ is parametrized by $\bar{n}$. Equation (5) means that, for each position withing the cycle, the data evolution along the cycles follows a smooth curve defined through a P^{th} order polynomial.

2.2 Local Synchronous Fitting

As previously pointed out, the estimation of the deterministic component resumes to find a curve that fits the data points that are related to the same location in the cycle. While the proposed approach also seeks a polynomial fit, this latter is made locally and for each data point. The adopted fitting method is excerpted from the "Savitzky-Golay filter" which is a widely known method to smooth or fit the data based on the least mean square solution of local polynomial fitting [10].

Precisely, for every $q \in \{1, \cdots, Q\}$, let's consider the data set $x_q[\bar{n}]$ being a function of q and parametrized by $\bar{n}$; we try to find the best LMS polynomial fit, with a fixed order P at the point $\bar{n}$, from the $2M+1$ subset centered at q, i.e. $\{x_{q-M}[\bar{n}], \cdots, x_{q+M}[\bar{n}]\}$. It follows that, this problem can be stated in a similar way as the previous subsection, i.e.:

$$(\forall q \in \{1, \cdots, Q\})\,(\forall \bar{n} \in \{1, \cdots, N\})\,\hat{\boldsymbol{b}}^{(q)}[\bar{n}] = \underset{\boldsymbol{b}^{(q)}[\bar{n}]}{\operatorname{argmin}} \|\boldsymbol{J}\boldsymbol{b}^{(q)}[\bar{n}] - \boldsymbol{x}^{(q)}[\bar{n}]\|^2 \tag{6}$$

where $\boldsymbol{x}^{(q)}[\bar{n}] = [x_{q-M}[\bar{n}], \cdots, x_{q+M}[\bar{n}]]^T$ represents the q^{th} subset, $\boldsymbol{b}^{(q)}[\bar{n}] = [b_0^{(q)}[\bar{n}], \cdots, b_P^{(q)}[\bar{n}]]^T$ are the $P+1$ polynomial coefficients associated with the q^{th} subset, and $\boldsymbol{J}$ the $(2M+1) \times (p+1)$ matrix such that for every $m \in$

$\{1, \cdots, 2M+1\}$, $p \in \{1, \cdots, P+1\}$, $\boldsymbol{J}_{m,p} = (m - M + 1)^{p-1}$. The $(2M+1)$-length curve that best fits the q^{th} subset writes:

$$s_m^{(q)} = \sum_{p=0}^{P} b_p^{(q)}[\bar{n}](m - M + 1)^p \tag{7}$$

It is worth noting that the window doesn't have to be symmetric in general, but it is decided to adopt in this paper a symmetric window centered on the sample itself, considering M samples on the left and M on the right. The Savitzky-Golay method suggests to estimate the deterministic component at the q^{th} data point by retaining the value of the polynomial at the central point i.e. at $m = M + 1$:

$$(\forall q \in \{1, \cdots, Q\})\,(\forall \bar{n} \in \{1, \cdots, N\}:) \quad \hat{d}[\bar{n} + (q-1)N] = \hat{s}_{M+1}^{(q)}[\bar{n}] = \hat{b}_{M+1}^{(q)}[\bar{n}] \tag{8}$$

It can be shown that solution of (6) writes:

$$(\forall q \in \{1, \cdots, Q\})\,(\forall \bar{n} \in \{1, \cdots, N\}) \quad \hat{\boldsymbol{b}}^{(q)}[\bar{n}] = \boldsymbol{H}\boldsymbol{x}^{(q)}[\bar{n}] \tag{9}$$

where $\boldsymbol{H} = (\boldsymbol{J}^T\boldsymbol{J})^{-1}\boldsymbol{J}^T$ is a matrix of size $(P+1) \times (2M+1)$ whose elements are independent of $\bar{n}$ and q. The $(M+1)^{th}$ element of the above vector namely $\hat{b}_{M+1}^{(q)}[\bar{n}]$ is actually a linear combination of $\boldsymbol{x}^{(q)}[\bar{n}]$ with the $2M+1$ elements of the $(M+1)^{th}$ row, $\boldsymbol{h}^T = [h_{-M}, \cdots, h_M]$, of $\boldsymbol{H}$ being independent of q and $\bar{n}$:

$$\hat{b}_{M+1}^{(q)}[\bar{n}] = \boldsymbol{h}^T\boldsymbol{x}^{(q)}[\bar{n}] \tag{10}$$

Considering Eqs. (8) and (9), one can write the estimate of the deterministic component, henceforth called "local synchronous fit" (LSF), as:

$$\begin{aligned}
\hat{d}[\bar{n} + (q-1)N] &= \sum_{m=-M}^{M} x_{q-m}[\bar{n}]h_m \\
&= \sum_{m=-M}^{M} x[\bar{n} + (q-1)N - mN]h_m \\
&= \sum_{i=-MN}^{MN} x[\bar{n} + (q-1)N - i]\tilde{h}_i
\end{aligned} \tag{11}$$

The above equation can be explained as follows: the deterministic component estimate at a given location $\bar{n}$ and a cycle N is a weighted sum of the data located at the same cycle positions in neighboring cycles. The number of considered cycles depends on the length of the S-G filter, being equal to $2M+1$: one for the sample located at the same position, M for the data located at the left (previous cycles) and M for the data located at the right (following cycles). With that being said, one can reformulate Eq. (11) as follows:

$$\hat{d}[\bar{n} + (q-1)N] = \sum_{i=-MN}^{MN} x[\bar{n} + (q-1)N - i]\tilde{h}_i \tag{12}$$

where $\tilde{\boldsymbol{h}}^T = [\tilde{h}_{-MN}, \cdots, \tilde{h}_{MN}]$ is obtained by zero-padding the S-G filter $\boldsymbol{h}$ as follows:

$$\begin{cases} \tilde{h}_i = h_m & \text{if } i = mN, \quad -M \leq m \leq M \\ \tilde{h}_i = 0 & \text{elsewhere} \end{cases} \tag{13}$$

Now applying the variable change $n = \bar{n} + (q-1)N$, Eq. (12) writes as:

$$\hat{d}[n] = \sum_{i=-MN}^{MN} x[n-i]\tilde{h}_i \tag{14}$$

The above formulation gives an interesting insight on the LSF method: it is equivalent to an LTI filtering with a $(2MN+1)$-length filter $\tilde{\boldsymbol{h}}$ whose coefficients are made of the associated $(2M+1)$-length S-G filter h zero-padded by $N-1$ samples among its coefficient.

It becomes obvious that the LSF turns to an LTI filtering of the original signal $x[n]$ with the $(2MN+1)$-length filter $\tilde{\boldsymbol{h}}$:

$$\hat{d}[n] = \sum_{i=-MN}^{MN} x[n-i]\tilde{h}_i \tag{15}$$

The fact that the LSF turns into a linear-time invariant convolution with $\tilde{\boldsymbol{h}}^T$ instead of fitting QN polynomial has a major impact on the computation time of the algorithm. Actually, this is a basic feature of the Savitsky-Golay (S-G) algorithm which, when applied to equally spaced data, is equivalent to an LTI convolution. It is important to note that, just like the S-G filter, the LSF filter $\tilde{h}$ is the same for P (P odd) and $P+1$, meaning that for a fixed M, $\tilde{h}$ is the same for $P=0$ and $P=1$, or $P=3$ and $P=4$.

3 Study of the LSF Filter

The previous section showed an intimate relationship between the S-G and LSF filters. The aim of this section is to study the time (or angle) and frequency (or order) domain properties of this filter.

3.1 Impulse Response

This section is concerned with the study of the impulse response (IR) of the LSF filter. A numerical simulation is made and displayed in Fig. 3 showing the IRs of the LSF filter for three polynomial orders ((a) $P=1$, (b) $P=3$ and (c) $P=5$) and three window lengths ($M=20$ (blue plot), $M=50$ (red plot) and $M=100$ (green plot)). The observations of these plots lead to the following properties:

– For $P=1$, the associated S-G filter is actually a moving average filter and the LSF in this case can be called as the "synchronous moving average".

- It is obvious that the non-zero coefficients are only defined at integer multiples of the fundamental period (since the plots are represented w.r.t. the fundamental period, it is equal to 1).
- The maximum value is located at zero meaning that the biggest weight is always associated with the center of the moving window. This is also a feature of a low-pass filter. For lower values of P, the first lobe tends to be flatter. The flattest one is that associated with $P = 1$ where the non-zero coefficients are all equal.
- For a fixed window width given by M, the maximum value of the coefficients decreases and the variability of the coefficient envelope increases with P, the reason is that further samples (within the $2M + 1$ window interval) are considered (through weights) as P increases, so that relatively higher frequency modulations are considered. This pattern is consistent with other values of M and P.
- For a fixed P, the shape of the envelope of the coefficients stays the same (to see this compare the three plots of the same color), yet further samples are naturally considered as the window width get larger with M. Of course the coefficient weight and location are adapted so that their squared sum equals 1.

Now having evaluated the IR shape, the next subsection evaluates its spectral properties.

3.2 Frequency Response Function

Reference [11] has studied the frequency response function (FRF) of the S-G filter which, as expected, turns into a low-pass filter whose cutoff frequency depends on both the polynomial order P and the window length through M. Equations (12) shows a strong relationship between the S-G filter $\boldsymbol{h}$ and the LSF filter $\tilde{\boldsymbol{h}}$. The spectral interpretation of this relationship is studied in this subsection as well as the spectral properties of the LSF filter. Let's define $H(\alpha)$ as the frequency response function (FRF) of the LSF filter of $\{h_i\}_{i=-M}^{i=M}$, that is

$$H(\alpha) = \sum_{i \in \mathbb{Z}} h_i e^{j2\pi i\alpha/N} \qquad -N/2 < \alpha \leq N/2 \tag{16}$$

where α is a frequency variable represented with respect to the fundamental order (i.e. associated with the fundamental cycle or period N) with unit [evt/rev], i.e. one event per revolution/cycle/period, i is the normalized angular index which represent i/N revolution of the fundamental period. The FRF of the LSF filter writes as:

$$\begin{aligned} \tilde{H}(\alpha) &= \sum_{k \in \mathbb{Z}} H(N(\alpha - k/N)) \qquad -N/2 < \alpha \leq N/2 \\ &= \sum_{k \in \mathbb{Z}} H(N\alpha - k) \qquad -N/2 < \alpha \leq N/2 \end{aligned} \tag{17}$$

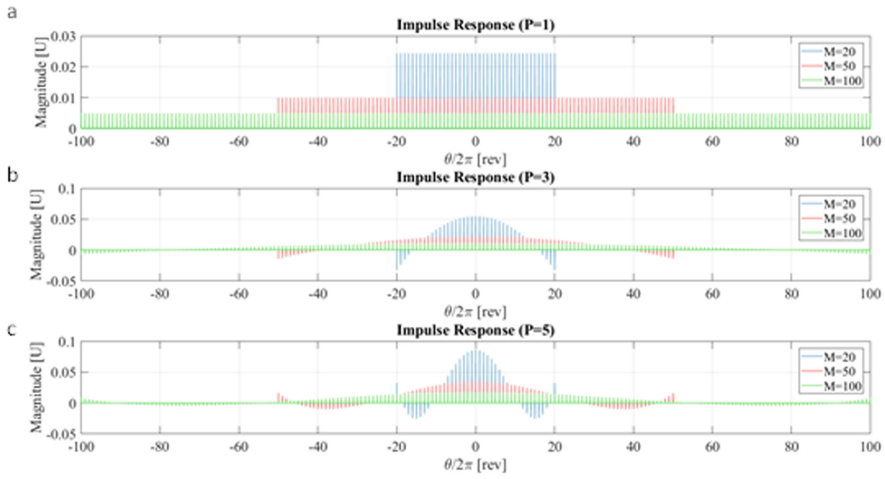

Fig. 1. The IRs of the LSF filter for three polynomial orders: (a) P = 1, (b) P = 3 and (c) P = 5. For each polynomial order, the IR is applied for three window length defined for M = 20 (blue plot), M = 50 (red plot) and M = 100 (green plot).

The above equation gives an interesting insight on the interpretation of the LSF filter, it is actually a comb-filter located at the fundamental order and all its harmonics i.e. the set of central frequencies is defined as: $\Omega = \{\alpha \in \mathbb{Z} \ \ s.t. \ \ -N/2 < \alpha \leq N/2\}$ (if N is odd, otherwise one sample on the left bound must be added just like the convention adopted in digital signal processing).

Similarly to the synchronous average, the comb-filter is made of N identical elementary low-pass filter $H(N\alpha)$ which, when shifted, turns into band-pass filter. This is due to the fact that the mean operation (which is the empirical average in the synchronous average case and the fitting in the LSF case) is made synchronously (across cycles). Interestingly, the elementary filter is nothing but the S-G filter FRF, defined for each couple (P, M), shrinked by a factor N (which is the number of samples per fundamental period). The reason of the spectral domain shrinkage is the zero-padding in Eq. (13) which spaces the sample by N (i.e. the IR of the S-G filter is dilated). A numerical simulation is made and displayed in Fig. 1 showing the IRs of the LSF filter for three polynomial orders ((a) $P = 1$, (b) $P = 3$ and (c) $P = 5$) and three window lengths ($M = 20$ (blue plot), $M = 50$ (red plot) and $M = 100$ (green plot)). The plots show a comb filter having a unit gain at the central frequencies and whose properties clearly depend on the both P and M (Fig. 2).

In order to study the effect of these parameters on the filter properties, it is more convenient to analyse the elementary filter which can be observed over a half of an order (for instance from 0 to 0.5) because of its symmetry. To do so, the FRFs of the LSF filter is computed for a fixed polynomial order $P = 3$, and for several window widths defined by $M = 20$ (blue plot), $M = 50$ (red plot), $M = 100$ (green plot) and $M = 100$ (black plot). The FRFs of the LSF filter is

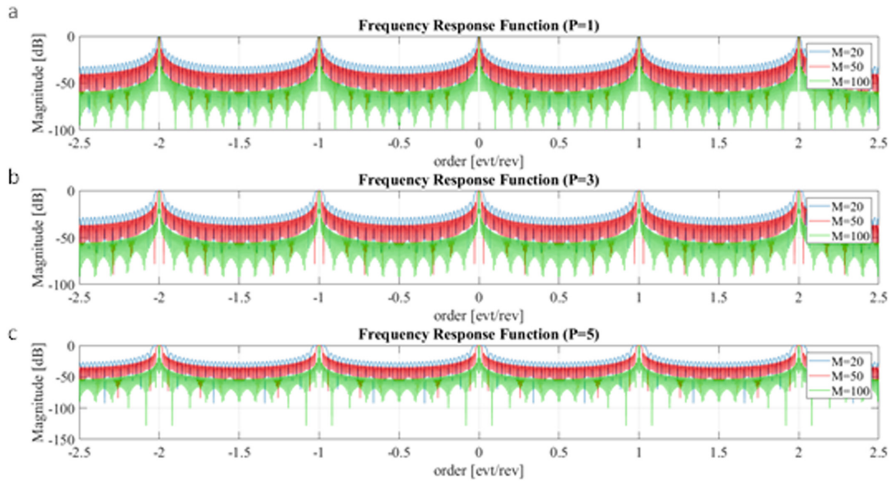

Fig. 2. The FRFs of the LSF filter for three polynomial orders: (a) $P = 1$, (b) $P = 3$ and (c) $P = 5$. For each polynomial order, the IR is applied for three window length defined for $M = 20$ (blue plot), $M = 50$ (red plot) and $M = 100$ (green plot).

also computed for $M = 50$: $P = 1$ (blue plot), $P = 3$ (red plot), $P = 5$ (green plot) and $P = 7$ (black plot).

The observations of these plots leads to the following properties of the elementary filter:

- Since the IR is real, $\tilde{H}(\alpha)$ is real and symmetric and so $H(N\alpha)$ also is.
- For $P = 1$, the associated S-G FRF is actually a sinc function, having the narrowest bandpass and the highest noise in the stop-band region for a fixed M.
- The cutoff frequency increases with P and decreases with M. The reason is that by increasing P for a given M or decreasing M for a given P, larger variations in the estimated component are allowed which results in higher frequencies of the modulations.
- The magnitude of the secondary lobes decreases with P and increases with M.

Since the filter bandpass is the most important element in choosing M and P, the 3-dB cutoff frequency is calculated w.r.t. M for five polynomial orders: $P = 1$, $P = 3$, $P = 5$, $P = 7$ and $P = 9$. Results are displayed in Fig. 4. The results are generally conform with what was stated previously. As expected, the cutoff frequency plots of higher polynomial order are located above the order plots associated with lower polynomial. It is remarkable how the cutoff frequency strongly decreases as M increases for lower values of M and this change gets slower for higher values until stabilizing asymptotically. Another feature not fully represented in these plots is the fact that almost any desired bandwidth can be obtained by multiple couples (M, P), disregarding the noise rejection properties

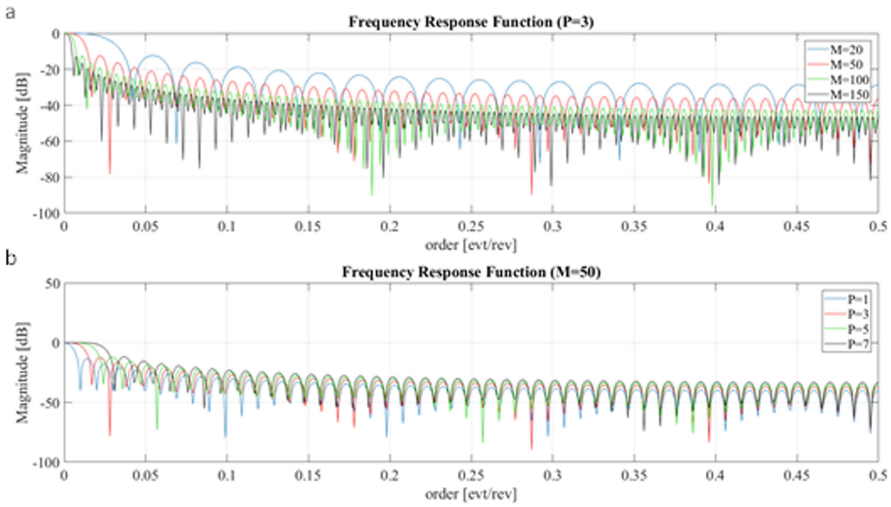

Fig. 3. (a)The FRFs of the LSF filter for $P = 3$: $M = 20$ (blue plot), $M = 50$ (red plot), $M = 100$ (green plot) and $M = 100$ (black plot). (b) The FRFs of the LSF filter for $M = 50$: $P = 1$ (blue plot), $P = 3$ (red plot), $P = 5$ (green plot) and $P = 7$ (black plot).

in the stopband region. In details, if one of these parameters is fixed, almost any cutoff frequency can be obtained by simply sweeping the other.

3.3 Authors' Recommendations on Parameter Setting

While the proposed method of Daher et *al.* [4] technique is parametrized by the polynomial order P, the LSF method is parametrized by the window width through M. The optimal parameter setting for a given problem depends on (i) the deterministic component itself through the variability of its complex envelope and (ii) the nature of the noise. In practice, neither the actual signal nor the noise statistics are known. This makes it hard to establish a systematic method for optimal parameter settings. However, according to the authors experience, it is proposed to fix the polynomial order to $P = 3$. The reason is that for $P = 1$ which corresponds to a synchronous moving average, the data tendency within the local window will not be considered, while higher values of P will not be useful since the window length defined by M can be shortened if higher polynomial values are required. Another way to see this, is the fact that almost any desired cutoff frequency can be obtained $(M, P = 3)$. The choice of M can be empirically set by the user by simply looking at the long-term modulations in the signal envelope: the variability of the latter has to be expressible with a 3 polynomial order.

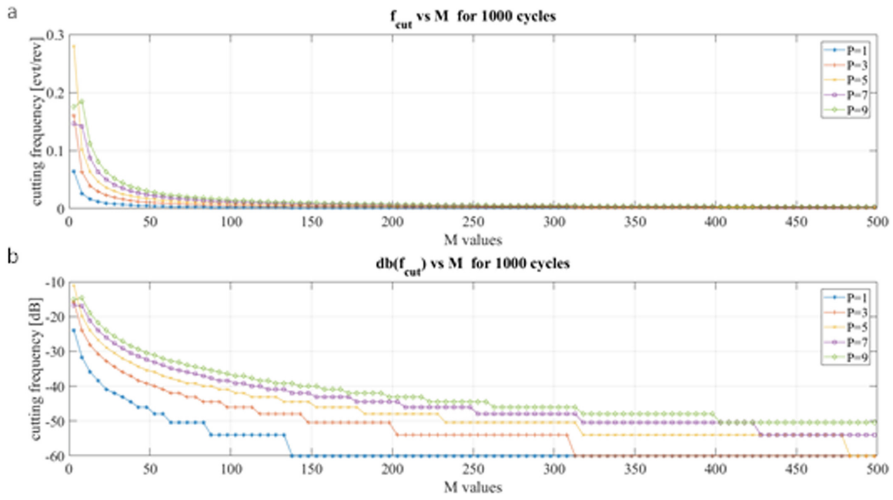

Fig. 4. (a) The 3-dB cutoff frequency w.r.t. M for various values of the window length defined by: $P = 1$(blue plot and $*$ markers), $P = 3$ (red plot and $+$ marker), $P = 5$ (orange plot and $\times$ marker), $P = 7$(purple plot and $\square$ marker) and $P = 9$ (green plot and $\diamond$ marker). (b) the dB representation of the plots in (a).

4 Application to Real Vibration Signal

In this section, the proposed approach is applied to analyze a helicopter vibration signal. The signal is measured on a two stage gearbox with an input pinion (L), two intermediate pinion (M) and (N) and an output pinion (O). The signal was acquired with a sampling frequency of $f_s = 65536$ Hz during 4 s. The kinematic of the reducer is presented in Table 1. The corresponding signal is displayed in Fig. 5 below. The rotating frequency increases from 63% to 100%.

Table 1. Characteristic order of the different pinion of the gearbox and the meshings.

Pinion	(L)	(M)	(N)	(O)
Order	1	0.293	0.293	0.1532
Meshing order	29		9.959	

The order spectrum of the vibration is displayed in Fig. 6. It exhibits mainly the characteristic order of the four pinion and two meshing order located at 2×9.959 and 29. The presence of those spectral line confirms that the gear signal is sinusoidal. Here, we focus on the meshing component 29 and its is estimated by the LSF filter. The latter is applied with a 3 order polynomial and with a window length of $M = 21$, $M = 101$ and $M = 401$ respectively. The provided estimation in time domain and time-frequency domain (spectrogram)

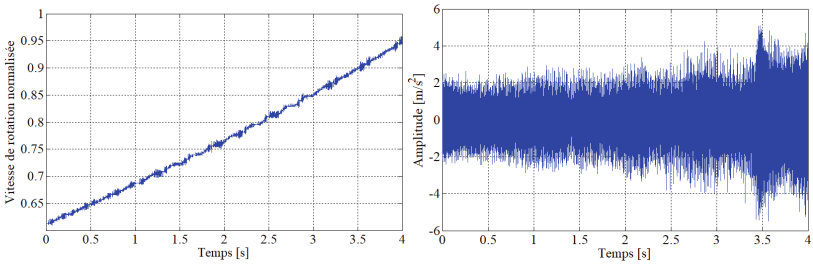

(a) Input pinion normalized rotating frequency.

(b) Gearbox vibration signal.

Fig. 5. Measured signals on the helicopter gearbox.

is presented in Fig. 7. It can be seen that whatever the window length(M), the LSF filter estimates component around order 29 and its harmonics. On the other hand, it can be seen in the time domain that the estimation is smoother for a larger window size. By decreasing M the LSF filter takes into account the modulations and higher frequencies. The spectrogram in Fig. 7 (c) shows a wide band estimate visible around the order 29 and its harmonics when the length of

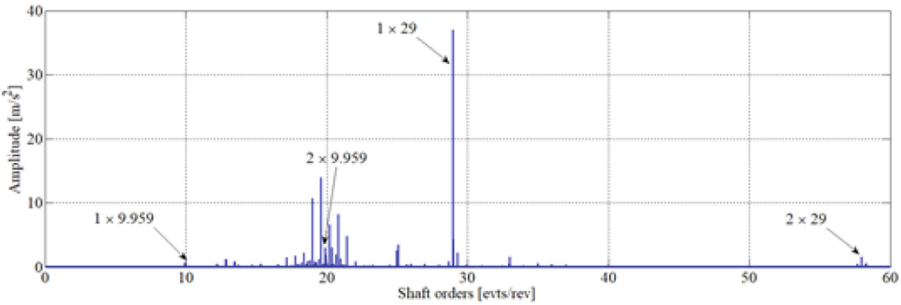

(a) Ordre spectrum between 0 to 60 evts/rev.

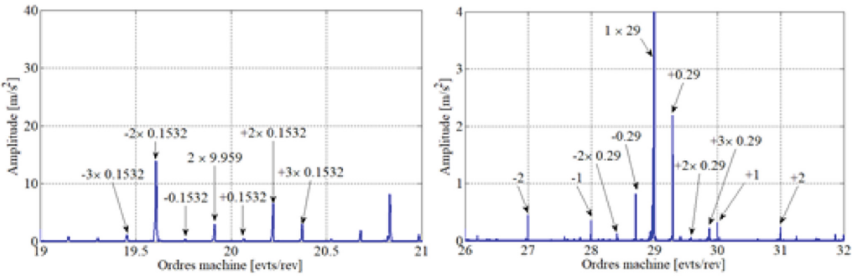

(b) Zoom around 20 evts/rev.

(c) Zoom around 29 evts/rev.

Fig. 6. Order spectrum of the raw gearbox vibration signal.

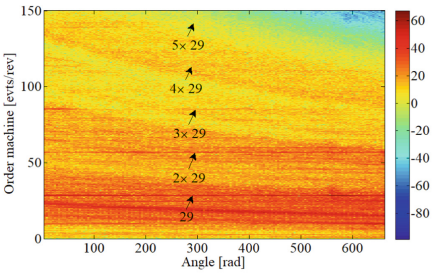

(a) Spectrogram of the raw signal.

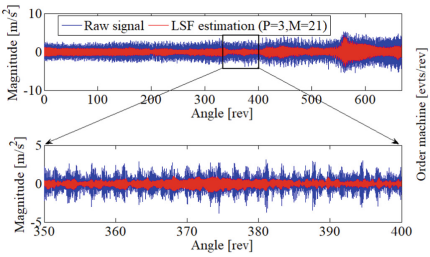

(b) Estimation for $P = 3$ and $M = 21$.

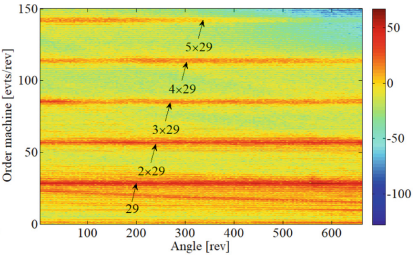

(c) Spectrogram of estimation in (b).

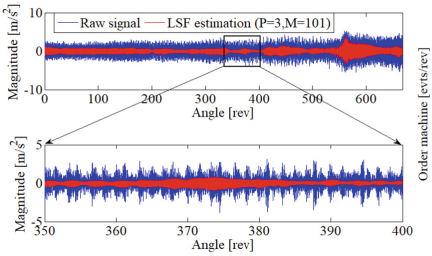

(d) Estimation for $P = 3$ and $M = 101$.

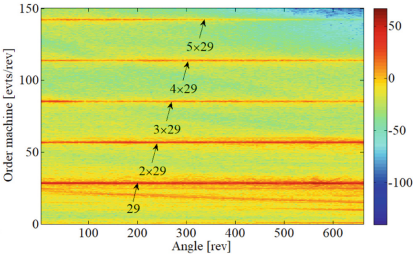

(e) Spectrogram of estimation in (d).

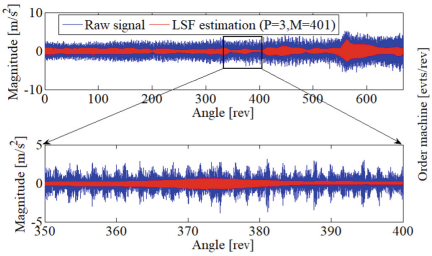

(f) Estimation for $P = 3$ and $M = 401$.

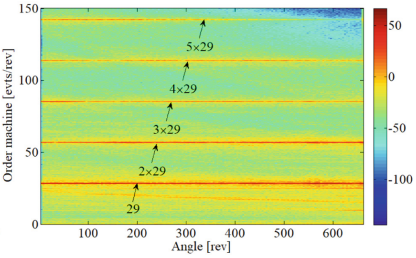

(g) Spectrogram of estimation in (f).

Fig. 7. Estimation of the meshing order 29 provided by LSF filter with a 3 order polynomial and different window length($M = 21, 101, 401$).

the window is equal to $M = 21$. The lateral bands come from the modulation of the meshing components by the rotation of the pinions (L) and (M). With regard to the spectrogram in Fig. 7 (e) and (g), the estimate provided by the LSF filter is narrow-band. The estimate is dominated mainly by the meshing components and the lateral bands are strongly attenuated. In addition to that, we observe that the noise level is strongly attenuated larger the size of the window is. These results on real signals are consistent with the theoretical study of the LSF filter of the Sect. 3. Based on these results, further analysis can be done such as pinion health monitoring by analyze the residual signal after removing the estimated meshing components.

5 Conclusions

This paper has studied the properties of the local synchronous fitting filter. It was shown that the impulse response of this filter is that of the classical Savitsky-Golay filter stretched by the number of point per cycle N and zero padded for all non-integer multiple samples of N. The frequency response function is a comb filter, being made of N identical elementary low-pass filters, which, when shifted, turns into narrow bandpass filters. The elementary filter is nothing but the SG filter of the same parameters, shrinked by a factor N. Further, the effect of the two main parameters, namely the window length M and the polynomial order P, is studied. It was shown that the cutoff frequency strongly decreases as M increases for lower values of M and this change get slower for higher values to reach an asymptote. Another interesting finding is the fact that any desired bandwidth can be obtained by fixing $P = 3$ and varying only M. This facts makes easier the manipulation of this method in practical applications.

Acknowledgement. Acknowledgement is made for the measurements used in this work provided through data-acoustics.com Database.

References

1. Ho, D., Randall, R.: Optimisation of bearing diagnostic techniques using simulated and actual bearing fault signals. Mech. Syst. Signal Process. **14**(5), 763–788 (2000)
2. Braun, S.: The synchronous (time domain) average revisited. Mech. Syst. Signal Process. **25**(4), 1087–1102 (2011)
3. McFadden, P., Toozhy, M.: Application of synchronous averaging to vibration monitoring of rolling element bearings. Mech. Syst. Signal Process. **14**(6), 891–906 (2000)
4. Daher, Z., Sekko, E., Antoni, J., Capdessus, C., Allam, L.: Estimation of the synchronous average under varying rotating speed condition for vibration monitoring. In: Proceedings of ISMA (2010)
5. Abboud, D., Antoni, J., Sieg-Zieba, S., Eltabach, M.: Deterministic-random separation in nonstationary regime. J. Sound Vib. **362**, 305–326 (2016)

6. Abboud, D., Assoumane, A., Marnissi, Y., El Badaoui, M.: Synchronous fitting for deterministic signal extraction in non-stationary regimes: application to helicopter vibrations. In: Surveillance, Vishno and AVE conferences. INSA-Lyon, Université de Lyon, Lyon, France (Jul 2019). https://hal.archives-ouvertes.fr/hal-02188704
7. Pan, M.-C., Wu, C.-X.: Adaptive Vold-Kalman filtering order tracking. Mech. Syst. Signal Process. **21**(8), 2957–2969 (2007)
8. Assoumane, A., Sekko, E., Antoni, J., Ravier, P.: Bearing signal enhancement using Taylor-h_∞ estimator under variable speed condition. IEEE Trans. Instrum. Meas. **67**(11), 2538–2547 (2018)
9. Roussel, J., Assoumane, A., Capdessus, C., Sekko, E.: Estimation of cyclic cumulants of machinery vibration signals in non-stationary operation. In: Timofiejczuk, A., Chaari, F., Zimroz, R., Bartelmus, W., Haddar, M. (eds.) Advances in Condition Monitoring of Machinery in Non-Stationary Operations. CMMNO 2016. Applied Condition Monitoring, vol. 9, pp. 21–31. Springer, Cham (2018). https://doi.org/10.1007/978-3-319-61927-9_3
10. Savitzky, A., Golay, M.J.: Smoothing and differentiation of data by simplified least squares procedures. Anal. Chem. **36**(8), 1627–1639 (1964)
11. Schafer, R.W.: On the frequency-domain properties of Savitzky-Golay filters. In: 2011 Digital Signal Processing and Signal Processing Education Meeting (DSP/SPE), pp. 54–59. IEEE (Jan 2011)